

# Microdomain structures with hyperbolic interfaces in block and graft copolymer systems

Hirokazu Hasegawa and Takeji Hashimoto\*

*Department of Polymer Chemistry, Graduate School of Engineering, Kyoto University, Kyoto 606-01, Japan*

and Stephen T. Hyde

*Department of Applied Mathematics, Research School of Physical Sciences, Institute of Advanced Studies, Australian National University, Canberra, ACT 0200, Australia*

*(Received 14 November 1995; accepted 5 January 1996)*

We have investigated a variety of polymer systems containing block or graft copolymers in order to search for new classes of microphase-separated structures other than the 'classical morphologies' such as lamellae, cylinders and spheres. The topological significance of these novel structures is that their interfaces have curvatures characteristic of hyperbolic surfaces. Systems exhibiting such structures can be divided into two groups: they are (a) polymer mixtures containing at least one block copolymer (e.g. block copolymer/homopolymer mixtures and block copolymer/block copolymer mixtures) and (b) block or graft copolymers with complex molecular architecture (e.g. star-block copolymers, graft-block copolymers, multicomponent multiblock copolymers, etc.). Copyright © 1996 Elsevier Science Ltd.

(Keywords: microdomain structures; block copolymer; graft copolymer)

## INTRODUCTION

In addition to popular morphologies, such as lamellae, cylinders and spheres, ordered bicontinuous morphologies, such as OBDD<sup>1,2</sup> and gyroid<sup>3</sup>, and mesh morphology<sup>4</sup> of microdomain structures have been detected in block copolymer systems. Those new morphologies belong to a new class of microdomain structures, whose interfaces are hyperbolic surfaces, and are important from both academic and industrial points of view. Mathematical modelling of microdomain interfaces with a variety of hyperbolic surfaces leads to predictions of a number of novel morphologies. In this paper we present some evidence for such structures and suggest a variety of ways—from simple to elaborate—to create such structures.

The standard classification of the microdomain morphology of block and graft copolymers consisted of three types, i.e. lamellae, cylinders and spheres. This scheme was established in the early stage of the history of block and graft copolymer studies<sup>5–9</sup>. Simple and familiar shapes from everyday life were introduced to explain the experimental observations. However, such a classification was largely a matter of convention only. In fact there was no theoretical support for such a limited range of morphologies. Even in the early stages, careful observations led some authors to suggest the possibility of bicontinuous network structures of high

symmetry<sup>9,10</sup>. It is now clear that a range of exotic morphologies other than lamellae, cylinders and spheres can occur<sup>1–4,11</sup>. An appropriate classification of microdomain morphologies, including these novel domain shapes, is necessary.

The microdomain morphology can be described by the shape of the interface between two phases, i.e. the local curvatures of the interface (the local aspect), and the topological continuity of the interface in space (the global aspect). Therefore, interfacial curvature is a key parameter to classify microdomain morphologies.

A curve has a well-defined curvature at each point, which corresponds to the inverse of the radius of a circle which most closely approximates the curve in the vicinity of the point of interest (called the osculating circle). The sign of the curvature depends on the location of the centre of the osculating circle: if it lies on the same side of the curve as the normal vector, it is positive (e.g. a convex curve), if the centre lies on the other side of the curve, it is negative (concave). Similarly, a surface has two principal curvatures which can be found at each point as follows (see *Figure 1*). A set of planes, all containing the normal vector to the surface at the point, intersects the surface in a set of planar curves, whose 'sectional curvatures' can be reckoned as for any planar curve. The most positive and most negative curvatures among all planar sections are the principal curvatures,  $k_1$  and  $k_2$ . These curves are always orthogonal. The Gaussian curvature ( $K$ ) of the surface at that point is equal to the product of these curvatures (with sign);

\* To whom correspondence should be addressed

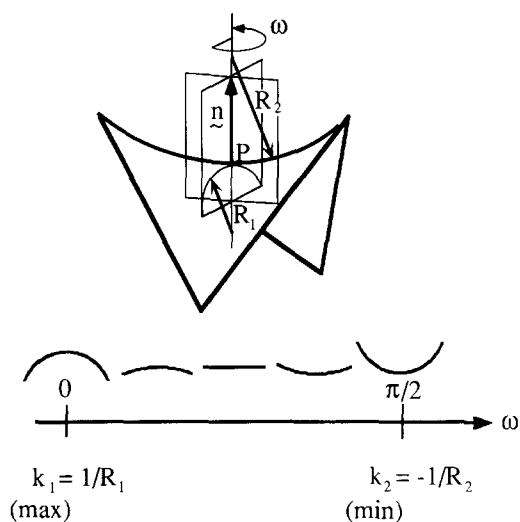


**Figure 1** The principal curvatures,  $k_1$  (maximum) and  $k_2$  (minimum) at a point P on a surface. In this example, the surface is a saddle, so the curvatures are positive and negative, respectively

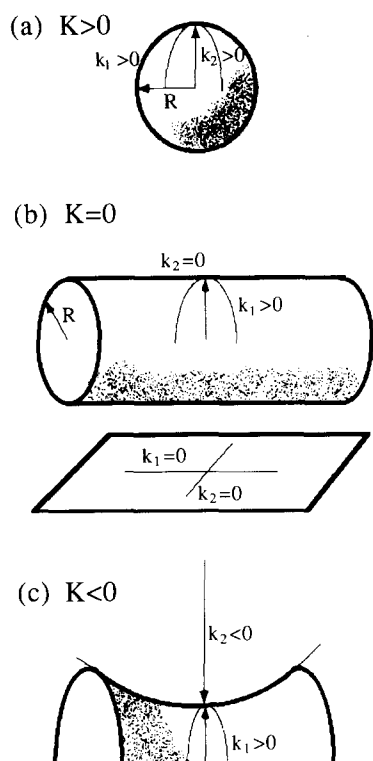


**Figure 2** Classification of surfaces by Gaussian curvature,  $K = k_1 k_2$ . (a) Elliptic surface ( $K > 0$ ), e.g. spheres:  $k_1 = k_2 > 0$ ; (b) parabolic surface ( $K = 0$ ), e.g. cylinders (upper):  $k_1 > 0$ ,  $k_2 = 0$  and planes (lower):  $k_1 = k_2 = 0$ ; (c) hyperbolic surface ( $K < 0$ ), e.g. saddle:  $k_1 > 0$ ,  $k_2 < 0$

the mean curvature ( $H$ ) is the average value of these curvatures.

$$K = k_1 k_2$$

and

$$H = (k_1 + k_2)/2$$

Surfaces can be classified into three broad categories, elliptic, parabolic and hyperbolic (see *Figure 2*), depending on the value of Gaussian curvature,  $K$ . Elliptic

geometry is characterized by positive Gaussian curvature, so that the surface is convex, or synclastic (*Figure 2a*). This includes spheres and ellipsoids. Parabolic surfaces have vanishing Gaussian curvature, so that one of the principal curvatures is zero (this curve is thus a straight line). This class includes planes and cylinders (*Figure 2b*). The geometry we shall deal with in this paper, hyperbolic surfaces, is characterized by negative Gaussian curvature, so that the surfaces are both concave and convex (principal curvatures of opposite sign), and are anticlastic, or saddle-shaped (*Figure 2c*). Minimal surfaces are characterized by zero mean curvature ( $H = 0$ ) at all points on the surface.

The conventional microdomain schema included only elliptic (spheres) and parabolic (cylinders and lamellae) geometries. However, there is no *a priori* reason to exclude hyperbolic geometries within the full schema. Bicontinuous microdomain structures—containing two interwoven continuous domains—are necessarily hyperbolic. The most homogeneous hyperbolic interfaces—with the smallest variations of Gaussian curvature—which do not intersect themselves (i.e. are ‘embedded’) and generate a bicontinuous morphology are the embedded triply-periodic minimal surfaces. The D surface is such a triply-periodic minimal surface. It bisects space into two identical, intertwined, continuous networks, whose tunnel axes in each network exhibit identical connectivity and geometry to the covalent bonding network in cubic diamond (hence the designation ‘D’). Each network has space-group symmetry  $Fd\bar{3}m$ . The minimal surface, which also contains symmetry elements relating the two labyrinths, displays  $Pm\bar{3}n$  symmetry. It thus offers a useful model to generate the ‘ordered bicontinuous double diamond’ (OBDD) morphology tentatively identified in some polymer systems. A detailed analysis will be reported elsewhere<sup>12</sup>. Other simple bicontinuous structures related to triply periodic minimal surfaces (assumed to be embedded) include the gyroid surface, consisting of two chiral networks (of opposite handedness), each of symmetry  $I4_32$ , (the actual minimal surface has symmetry group  $Ia\bar{3}d$ )<sup>3</sup> and the P-surface, containing identical labyrinths, each of symmetry  $Pm\bar{3}m$  (surface symmetry  $Im\bar{3}m$ ). Since more than 30 triply-periodic minimal surfaces, of various symmetries and topologies, have been reported to date<sup>13–15</sup>, a variety of bicontinuous microdomain structures characterized by those surfaces may be physically accessible to polymer systems. In addition to these triply periodic structures, a variety of double-periodic surfaces, containing both elliptic and hyperbolic regions, called ‘mesh’ surfaces<sup>4</sup>, are germane to polymer self-assembly. Further non-classical interfacial shapes, such as constricted cylinders and wavy lamellae<sup>16</sup>—which also have local patches of hyperbolic form—can be envisaged. In some cases, these forms can be generated from simple deformation of triply-periodic minimal surfaces<sup>4</sup>.

## EXPERIMENTAL

We have examined the microdomain morphology of a variety of polymer samples, either synthesized by ourselves or supplied by our collaborators. The technique we employed to judge the bicontinuity of the microdomain was transmission electron microscopy of

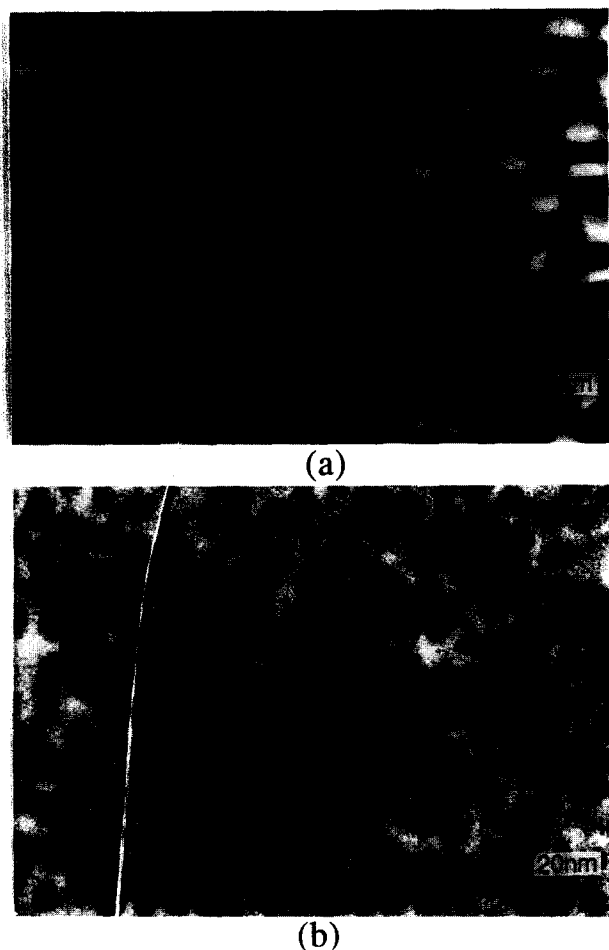


**Figure 3** (a) Electron micrograph of an ultrathin section cut from a toluene-cast film of 80:20 (wt%/wt%) mixture of HY-12 (SI diblock copolymer) and HI-3 (PVME) stained with OsO<sub>4</sub>, exhibiting lamellar-catenoid structure. (b) Electron micrograph of an ultrathin section cut from a toluene-cast film of 70:30 (wt%/wt%) mixture of HY-1 (SI diblock copolymer) and HI-3 stained with OsO<sub>4</sub>, showing the characteristic 'wagon wheel' pattern of the OBDD structure

ultrathin sections of the cast films from solutions in neutral solvents. A Hitachi H-600 transmission electron microscope (EM) with accelerating voltage of 100 kV and an LKB 4800A Ultratome were used. The OBDD, gyroid, or related structures<sup>1-3</sup> can be identified by characteristic 'wagon wheel' patterns, of approximate 3- or 6-fold rotational symmetry, provided sections of appropriate crystallographic orientation can be seen in the EM. However, in general, it is not easy to distinguish bicontinuous or mesh morphologies from more classical morphologies of elliptic or parabolic geometry (especially cylinders), as the electron microscopic images change dramatically with the sectioning direction (or angle) through the structure, section thickness and observation angle (i.e. the tilt of the sample stage of the electron microscope). We have developed a computer program for the simulation of the electron microscopic images of various microdomain morphologies including bicontinuous structures and simple morphologies (such as cylinders and spheres) as a function of the sectioning direction, section thickness and observation angle<sup>12,17</sup>. This simulation procedure significantly aids the detection of microdomain morphology, as typical sections of bicontinuous morphologies are very complex. We have also found that hexagonally packed cylinders

can result in complex patterns, sometimes resembling those of a bicontinuous structure. Detailed analysis will be published elsewhere<sup>12</sup>. Therefore, assignment of morphology, specially in bicontinuous cases, must be done cautiously.

## RESULTS

The polymeric systems in which bicontinuous morphologies were observed were: (1) AB block copolymer/C homopolymer mixtures, (2) block copolymer/block copolymer mixtures, (3) multicomponent copolymers, (4) star block copolymers, (5) graft-block copolymers, and (6) tapered-block copolymers.

### *AB block copolymer/C homopolymer mixtures*

Winey *et al.*<sup>18</sup> have investigated extensively mixtures of AB block copolymer and A homopolymer to determine the composition range of the OBDD morphology. They used polystyrene-*block*-polyisoprene (SI) and polystyrene-*block*-polybutadiene (SB) as AB block copolymers, and polystyrene (PS), polyisoprene (PI) and polybutadiene (PB) homopolymers. They successfully obtained the OBDD morphology for certain pairs of the blends although their composition range for the morphology (64–67 vol% PS) was as narrow as that (62–66 vol% PS) we found in neat SI linear diblock copolymers<sup>1</sup>. Spontak *et al.* examined the range of molecular weight of PS block and its ratio to that of PS homopolymer in the OBDD-forming SI diblock copolymer/PS homopolymer blends with a fixed bulk composition of 66 vol% PS<sup>19</sup>.

When component A and component C are miscible in AB block copolymer/C homopolymer blends, homopolymer C may be solubilized in the A microdomain of the block copolymer in the strong segregation regime of the block copolymer. Solution-cast films of AB block copolymer/C homopolymer mixtures may exhibit uniform microdomain structures without liquid-liquid phase separation between AB block copolymer and C homopolymer in a limited range of blend compositions<sup>20-22</sup>. Bicontinuous morphologies can also be expected for such systems. In fact, we have reported a bicontinuous structure lacking long-range order, found in a film of 80:20 (wt%/wt%) mixture of SI diblock copolymer (HY-12:  $M_{n,total} = 5.24 \times 10^5$ ,  $M_w/M_n = 1.16$ , PS/PI = 52:48 wt%/wt% = 49:51 vol%/vol%) and poly(2,6-dimethylphenylene oxide) (PPO:  $M_n = 1.17 \times 10^4$ ,  $M_w/M_n = 3.64$ ) prepared by quick casting of 10% solution in toluene<sup>20</sup>. In this case, the interface between the PI and PS/PPO domains has appreciable mean curvature: it is curved more towards the PI domains than the PS/PPO domains. Thus, the PI microphase forms a three-dimensional network and the microphase of PS/PPO mixture forms the matrix. Xie *et al.* reported the observation of the OBDD structures in the blends of polystyrene-*block*-polybutadiene-*block*-polystyrene triblock copolymer and poly(vinyl methyl ether) (PVME) over the composition range of 33–37 vol% of mixed phase of PS and PVME<sup>23</sup>.

Here, we would like to show two more examples. The neat block copolymers adopt a lamellar morphology for both cases. *Figure 3a* shows an electron micrograph of an ultrathin section cut from a solution-cast film, with toluene as a solvent, of an 80:20 (wt%/wt%) mixture of

HY-12 (the same SI diblock copolymer as above) and PVME (HI-3:  $M_n = 2.7 \times 10^4$ ,  $M_w/M_n = 1.40$ ) stained with osmium tetroxide ( $\text{OsO}_4$ ). The film exhibits microdomains throughout the specimen, with no evidence for macroscopic segregation of PVME. The structure in Figure 3a resembles the 'lamellar catenoid' structure, a bicontinuous microdomain structure reported by Thomas *et al.*<sup>11</sup> and Spontak *et al.*<sup>19</sup> The structure proposed by Thomas *et al.*<sup>11</sup> consists of alternating dark and light layers. Each layer of one phase contains catenoid-shaped channels of the other phase which are connected to the neighbouring layers: in principle any anisotropic triply periodic hyperbolic surface can display such a structure in the appropriate orientation(s). The catenoidal channels appear bright in the dark layers and dark in the light layers in the micrograph. Thus, both phases are continuous in three dimensions. While the domain geometry of our system exhibits similarities to their model, it contains important differences. Detailed analysis of this structure will be presented elsewhere<sup>22</sup>.

Figure 3b was obtained for 70:30 (wt%/wt%) mixture of another SI diblock copolymer (HY-1:  $M_{n,\text{total}} = 3.5 \times 10^4$ ,  $M_w/M_n = 1.03$ , PS/PI = 55:45 wt%/wt% = 52:48 vol%/vol%) and HI-3. This cast film exhibited coexistence of two kinds of microdomain structures: PI cylinders and the OBDD structure of PI networks. No isolated PVME phase was found. The electron microscopic image shown in Figure 3b is concerned with one kind of microdomain, showing the typical wagon wheel pattern (marked by white dashed lines) of the OBDD structure, which is observed in the section cut parallel to the (111) planes of the double-diamond lattice. The dark 'wagon wheels' in the micrograph correspond to the two PI diamond networks.

In contrast to the observation by Winey *et al.*<sup>18</sup> we observed the bicontinuous microdomain morphologies for a significantly wide range of compositions in the SI diblock copolymer/PVME mixtures. The volume fraction of the mixed phase of PS and PVME in HY-12/HI-3 80:20 mixture and HY-1/HI-3 70:30 mixture was 0.59 and 0.65, respectively, according to our calculations, using a density of 1.052 for PS<sup>1</sup>, 0.925 (vinyl rich, HY-12) or 0.913 (1,4-rich, HY-1) for PI<sup>1,24</sup>, and 1.047 for PVME<sup>25</sup>. Thus, it appears that bicontinuous structures can be formed over a wider range of compositions in AB block copolymer/C homopolymer mixtures than in AB block copolymer/A homopolymer mixtures. It should be noted that the molecular weight of HI-3 (PVME) is larger than that of the PS block chain of HY-1. In the case of SI diblock copolymer/PS homopolymer mixtures, the PS homopolymer does not swell the PS block chains and the lamellar morphology is expected to remain unchanged if the homopolymer molecular weight is comparable to or greater than that of the corresponding block chains ('dry brush' regime)<sup>26,27</sup>. The apparent transition from lamellae to OBDD by adding PVME suggests swelling of the PS block chains by the PVME homopolymer. This may be explained by better affinity (negative  $\chi$ )<sup>25</sup> between PS and PVME than that between PS block chain and PS homopolymer.

We have also observed the coexistence of cylindrical and OBDD morphologies, found in a HY-1/HI-3 70:30 mixture. In this case there is a possibility of macrophase

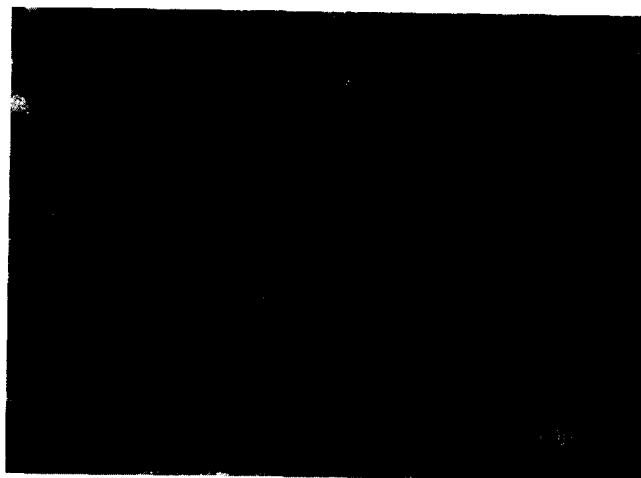


Figure 4 Electron micrograph of an ultrathin section cut from a toluene-cast film of 50:50 (wt%/wt%) mixture of two SI block copolymers, HK-7 and HS-10 stained with  $\text{OsO}_4$ , exhibiting an OBDD morphology with the PS diamond networks indicated by dashed lines

separation between HY-1 and HI-3 during solvent evaporation. The concentration fluctuations induced by spinodal decomposition may cause the spatial variation of microdomain morphology, as detected in films containing HY-12/PPO mixtures cast slowly from toluene solutions<sup>20</sup>. Winey *et al.*<sup>18</sup> also reported the observation of the coexistence of two morphologies, lamellar and cylindrical, although no macrophase separation was expected for their mixtures.

#### Block copolymer/block copolymer mixtures

Schwieger *et al.*<sup>28</sup> have reported that a solution-cast film (with toluene) of a mixture of three SIB diblock copolymers with different PS/PB ratios and molecular weights exhibits a bicontinuous morphology, namely a disordered three-dimensional network of PB phase in the PS matrix. In their case, the volume fraction of PS in the mixture was 0.75, which is far from the ordinary composition range of the bicontinuous structure. The same mixture had the morphology of PB cylinders in PS matrix, when it was cast from solution in a mixed solvent of tetrahydrofuran (THF) and methylethylketone (MEK), which has poor affinity with the PI component. They also showed that the bicontinuous morphology is superior to the cylindrical morphology in terms of mechanical properties.

The change of microdomain structures with composition in block copolymer/block copolymer mixtures was studied by Hadziioannou and Skoulios<sup>29</sup> by means of small-angle X-ray and neutron scattering. They reported the morphological transition from lamellae to cylinders for binary mixtures of block copolymers which show lamellar and cylindrical morphologies on their own. This result seems to be reasonable. We have also studied microdomain structures in SI block copolymer/SI block copolymer mixtures by means of small-angle X-ray scattering and electron microscopy. The results of our study have been discussed elsewhere<sup>30</sup>. In the course of this study, however, we observed a peculiar phenomenon. The toluene-cast film of 50:50 (wt%/wt%) mixture of two SI block copolymers (HK-7:  $M_{n,\text{total}} = 3.19 \times 10^4$ ,  $M_w/M_n = 1.09$ , PS/PI = 35:65 wt%/wt% = 32:68 vol%/vol%, and HS-10:  $M_{n,\text{total}} = 8.14 \times 10^4$ ,



**Figure 5** Electron micrograph of an ultrathin section cut from a toluene-cast film of polyisoprene-*block*-polystyrene-*block*-polyisoprene-*block*-poly(4-vinylbenzyl dimethylamine)-*block*-polyisoprene three-component pentablock copolymer (TUN-1003) cast from toluene solution stained with OsO<sub>4</sub>, showing the 'wagon wheel' pattern of the OBDD structure

$M_w/M_n = 1.13$ , PS/PI = 63 : 37 wt%/wt% = 60 : 40 vol%/vol%—both of which adopt a lamellar morphology in their neat films—exhibits an OBDD (or related) structure, as shown in the electron micrograph of Figure 4. The volume fraction of PS in the mixture was 0.46 which is again far from the composition range (28–33 vol%<sup>18</sup> or 62–66 vol% PS<sup>1</sup>) of the bicontinuous structure in neat SI linear diblock copolymers. In this case bright PS microdomains form the diamond networks, indicated by dashed lines in the matrix of PI microphase. The same specimen also contains the morphology with PI cylinders as the 50 : 50 mixtures of HY-1/HI-3 described in the previous section. The reproducibility of this phenomenon has been confirmed.

#### Multicomponent multiblock copolymers

The microdomain morphologies of ABC<sup>31–34</sup> or ABACA-type<sup>35</sup> linear three-component multiblock copolymers have been investigated by several research groups. Three-component multiblock copolymers can exhibit a greater variety of morphologies than two-component block copolymers. For example, in addition to the single morphologies such as lamellae of three planar phases with ABCB repeat sequences, AB coaxial cylinders in a C matrix and spheres with an A phase core and a B phase shell in a C matrix, a combination of two morphologies, such as AB alternating lamellae with C spheres in B layers, has been reported. However, these analyses were all based on the three classical morphological types: lamellae, cylinders and spheres.

Mogi *et al.*<sup>36</sup> observed another type of OBDD structure in polyisoprene-*block*-polystyrene-*block*-poly-2-vinylpyridine triblock copolymers. According to their observations by electron microscopy each of the PI and poly-2-vinylpyridine (P2VP) microphases forms one of the diamond networks of the OBDD structure and the interstitial hyperbolic sheet separating the networks is filled with PS. Therefore, all three phases are continuous in three dimensions, accordingly they named this structure the 'OTDD' (ordered tricontinuous double diamond) structure. The volume fraction of PS for this structure was 0.48–0.59 and the PI and P2VP microphases have nearly equal volume fractions.

We too have found the OBDD (or related) morphology in such a complex system<sup>37</sup>. Figure 5 shows an electron micrograph of polyisoprene-*block*-polystyrene-*block*-polyisoprene-*block*-poly(4-vinylbenzyl dimethylamine)-*block*-polyisoprene three-component pentablock copolymer (TUN-1003:  $M_{n, total} = 1.94 \times 10^5$ ) cast from a solution in toluene. The weight fraction of each block was 0.09, 0.38, 0.07, 0.38 and 0.08, respectively. Since the ultrathin section was stained with OsO<sub>4</sub>, the PI and

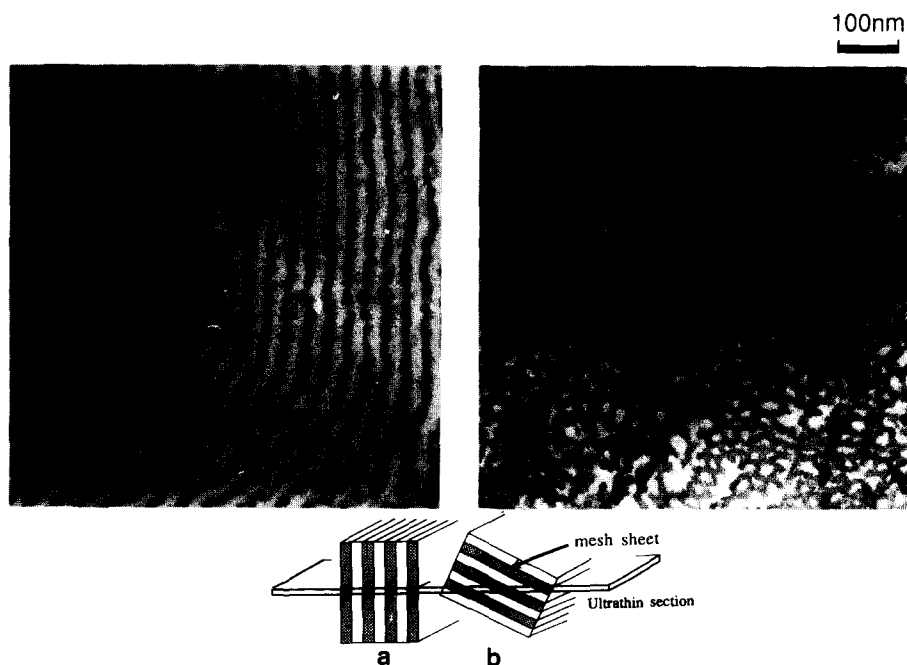


**Figure 6** Electron micrographs of the OsO<sub>4</sub>-stained ultrathin section of toluene-cast film of 70:30 wt%/wt% blend of polystyrene-*block*-polybutadiene radial block copolymer (KR03) and polystyrene (TS23) exhibiting a mesh morphology: ultrathin sections cut perpendicularly (a) and parallel (b) to the film surface corresponding to the sections normal and oblique to the mesh sheets, respectively, as illustrated in the insertion

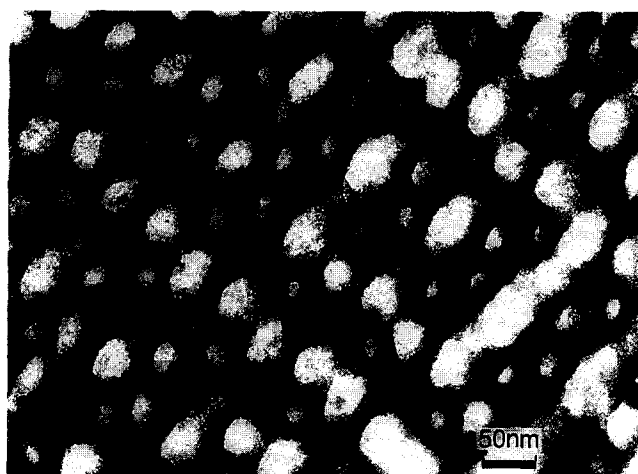


**Figure 7** Electron micrographs of the OsO<sub>4</sub>-stained ultrathin section of benzene-cast film of polystyrene-*block*-(poly-4-vinylphenyldimethylvinylsilane-*graft*-polyisoprene) (YSF-12), exhibiting a new type of bicontinuous morphology

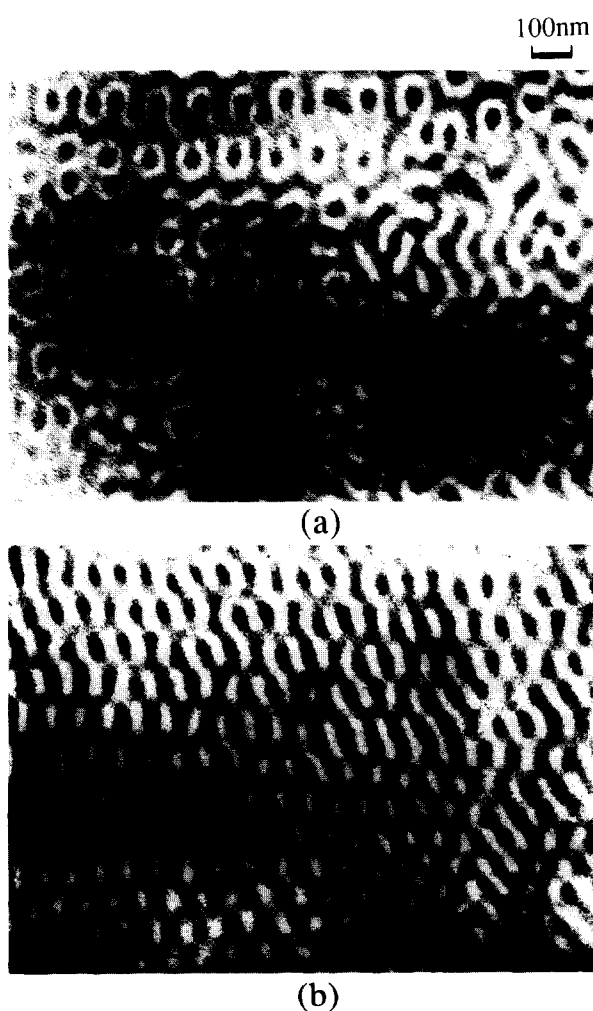


**Figure 8** Electron micrographs of the OsO<sub>4</sub>-stained ultrathin section of toluene-cast film of SI tapered-block copolymer (TB-3), exhibiting a bicontinuous morphology

poly(4-vinylbenzyl)dimethylamine (P4VBDM) components appear dark in the micrograph<sup>32</sup>. Figure 5 shows a typical wagon wheel image, characteristic of the OBDD or related structures, indicated by the white dashed

lines. From detailed analysis<sup>37</sup> it is clear that the OBDD networks consist of inner P4VBDM microphase and outer PI microphase. The PS microphase fills the hyperbolic sheet between the networks, rather than the networks themselves, despite the fact that its volume fraction is only 0.33.

It should be noted that some new complicated morphologies were recently reported by Stadler *et al.* for ABC triblock copolymers<sup>38</sup>.

#### Star block copolymers

Star (or radial) block copolymers have a non-linear molecular architecture, i.e. more than three diblock copolymers are bundled at one end by covalent bonds. The wagon wheel pattern which was analysed by Thomas *et al.*<sup>2,11</sup> was first observed by Aggarwal<sup>39</sup> for an SI star block copolymer having 15 arms on average and 30 wt% PS. Thomas *et al.* observed the formation of the OBDD structure for SI star block copolymers with PS volume fractions of 0.27–0.38 (ref. 40). In these cases PS forms double diamond networks and PI forms the matrix.

We have observed a bicontinuous morphology in 60:40 (wt%/wt%) mixtures of an SB star block copolymer (KR-03, Phillips Petroleum Co.,  $M_{n,\text{total}} = 8.0 \times 10^4$ ,  $M_w/M_n = 1.96$ , PS/PB = 24 : 76, four arms on average) and PS homopolymer (TS23, TOSOH Co., Ltd,  $M_n = 2.8 \times 10^3$ ,  $M_w/M_n = 1.05$ )<sup>4</sup>. The volume fraction of PS in the mixture is estimated to be 0.73. The microdomain morphology of neat KR-03 is lamellar, indeed we have not observed a bicontinuous morphology in the neat star block copolymer. In the 70:30 mixture we have found a 'mesh' structure (Figure 6)<sup>4</sup>. This morphology is not a bicontinuous structure since the three dimensional mesh morphology is generated by stacking of discrete mesh layers. Figure 6 (a, b) corresponds to the sections normal and oblique to the mesh sheets, respectively, as illustrated in the inset.

#### Graft-block copolymers

Graft copolymers are typical examples of copolymers having block sequences and nonlinear architecture which also exhibit microphase separation in the segregation regime. A sophisticated technique was developed to control the number and molecular weight of the branches<sup>41</sup>. Since AB block copolymers with a controlled number of functional groups in B block are synthesized first, followed by the growth or coupling of C chains on the B blocks, the final product is called a 'graft-block copolymer'<sup>41</sup>. Figure 7 shows an electron micrograph of the OsO<sub>4</sub>-stained ultrathin section of solution-cast film (with benzene) of polystyrene-*block*-(poly-4-vinylphenyldimethylvinylsilane-*graft*-isoprene) (YSF-12:  $M_{n,\text{total}} = 4.3 \times 10^5$ ,  $M_{n,\text{PS}} = 2.4 \times 10^5$ ,  $M_{n,\text{PI}} = 1.8 \times 10^4$ , 10 branches/chain on average) kindly supplied by the late Professor T. Fujimoto. The molecular architecture of this polymer resembles a toothbrush, i.e. the PI chains are grafted only on the very short poly-4-vinylphenyldimethylvinylsilane (PVPDVS) block chain which is connected to one end of the PS chain. Therefore, PVPDVS block chains are unable to form an independent microdomain on their own, and may be located at interfaces between the PS and PI microdomains. Thus, YSF-12 should essentially exhibit a microdomain structure of the two-phase system consisting of a (dark) PI phase and a (light) PS phase. This implies that the gray

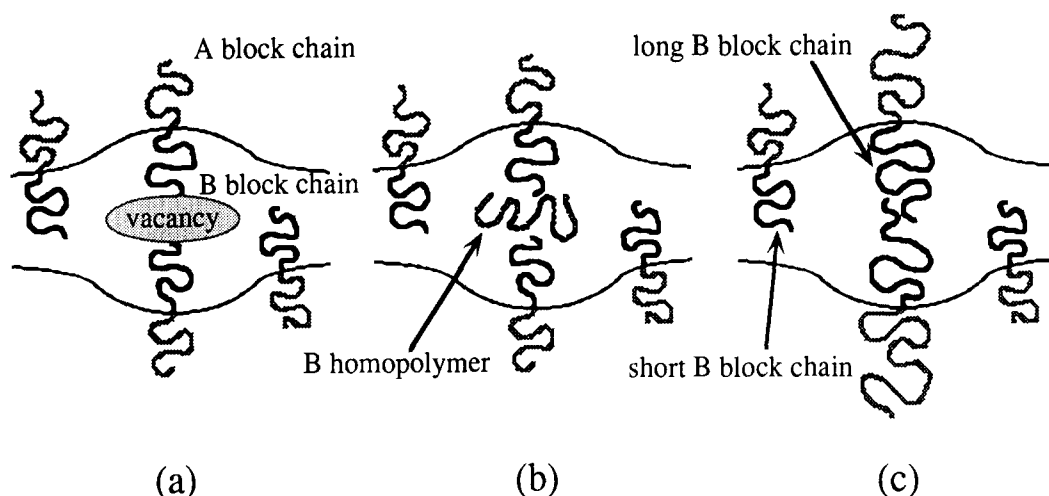


**Figure 9** Schematic illustration of the packing of the block chains in a bicontinuous microdomain structure. (a) Neat block copolymer system. Block chain A must be more stretched than block chain B. (b) Block copolymer/homopolymer mixture. Space in the centre is filled with homopolymers. (c) Block copolymer/block copolymer mixture. (A) Long block chains; (B) short block chains

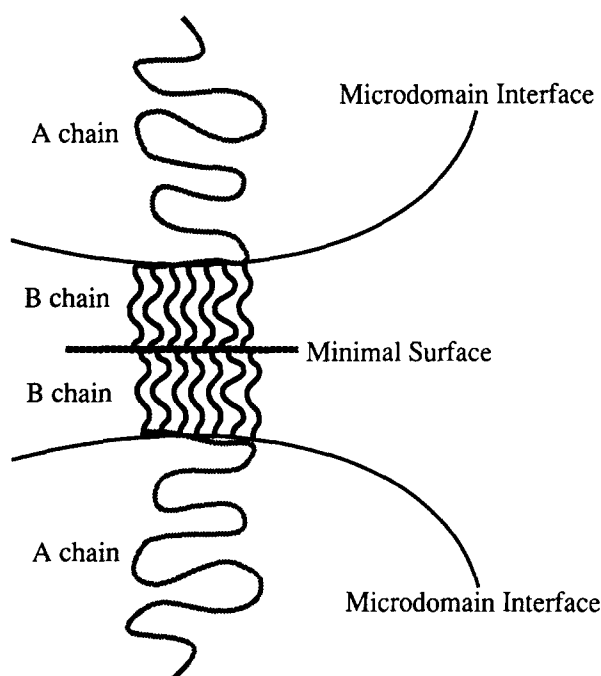


**Figure 10** Schematic illustration of the packing of the graft-block copolymer in a bicontinuous microdomain structure. The densely packed grafted chains form a bimolecular sheet on a 3D periodic minimal surface and more flexible long block chains form a pair of interwoven 3D networks

region observed in the EM image is due to projection through both PS and PI microdomains. The micrograph shows a peculiar pattern, revealing a periodic bicontinuous structure which cannot be explained by reported bicontinuous structures such as the OBDD, gyroid or 'lamellar catenoid'. Analysis of this structure is in progress.

#### Tapered-block copolymers

SI tapered-block copolymers are linear block copolymers in which the composition (the content of isoprene and styrene monomers) varies continuously from one end to the other along the copolymer chain. The concentration of isoprene monomeric units gradually

increases along the chain. The synthesis technique is described elsewhere<sup>42</sup>. These copolymers also undergo microphase separation, although their mechanical properties are quite different from ordinary SI block copolymers<sup>42</sup>. Figure 8 shows the electron micrographs of the OsO<sub>4</sub>-stained ultrathin section of toluene-cast film of SI tapered-block copolymer [TB-3:  $M_{n,total} = 1.06 \times 10^5$ ,  $M_w/M_n = 1.09$ , styrene content 45 wt% (42 vol%)]. The microdomains clearly form the OBDD or related structure, where the PI-rich domains form the interwoven networks, separated by a PS-rich matrix—evidenced by the characteristic wagon wheel pattern (Figure 8a). The rectangular lattice pattern with vague horizontal lines and distinct vertical lines in part b of the figure can be recognized as the [211] projection of the double diamond lattice<sup>1,2</sup>.

## DISCUSSION

### Characteristics of the systems exhibiting bicontinuous structures

We have observed bicontinuous morphologies in a wide range of polymeric systems. These include AB block copolymer/C homopolymer mixtures, block copolymer/block copolymer mixtures, multicomponent multiblock copolymers, star block copolymers, graft-block copolymers, and tapered-block copolymers. To date, these complex systems have not been investigated as frequently as ordinary systems, such as neat AB diblock or ABA triblock copolymers. Nevertheless, we have observed bicontinuous morphologies as frequently as other morphologies in these more complex systems. These systems apparently form a bicontinuous microdomain morphology over a wider range of compositions than found in simple systems. This fact implies that the former systems have a greater tendency to form bicontinuous morphologies than the latter.

At a theoretical level, these apparently disparate observations can be collected into two phenomena. First, the studies of mixed systems suggest that the admixture of extra polymeric components to homogeneous copolymer aggregates seems to promote the formation of bicontinuous domains. This result has

been theoretically predicted elsewhere<sup>43</sup> in the strong-segregation regime of linear diblock copolymer self-assembly. The prediction was made by reconciling local and global constraints in ideal strongly segregated rubber-like polymer systems. If the conformational entropy of the copolymer chains is maximized as a function of the principal curvatures of the interface between the domains, the results depend strongly on the global geometric constraints imposed on the system by its composition. If the copolymer can adopt its optimal curvatures expected from local entropic constraints (i.e. the global and local constraints are compatible), we expect the formation of hyperbolic interfaces—which may lead bicontinuous domains—over a significant range of diblock compositions. (This range extends from about 30% by volume of the minor block, up to almost equal block volumes.) This local optimization gives the 'spontaneous' or 'preferred' curvatures of the interface. However, global constraints often prevent the adoption of these spontaneous curvatures. For example, in pure diblock copolymer systems, the relative volume requirements of each domain cannot be satisfied if the system takes up its spontaneous curvatures. In this pure system then, the formation of a bicontinuous morphology (or any hyperbolic geometry, including the mesh architecture) is strongly suppressed.

#### *Principles to produce bicontinuous microdomain structures*

The effect of adding extra components to the system is to relax these global constraints. For example, the presence of homopolymer allows the formation of a range of curvatures by the interface between the blocks, since voids in the resulting global domains (Figure 9a) can be filled with homopolymer (Figure 9b). A similar effect is expected using block copolymers with a distribution of block chain-lengths (Figure 9c). In both cases, the system is able to relax the global constraints, so that the interface can move towards its preferred curvatures with the assistance of the polymeric additives, which act as molecular 'fillers' (Figure 9). A further geometric constraint must also be considered in this context, namely the ability of the system to adjust to the curvature inhomogeneities which are required in all global realizations of hyperbolic interfaces which are free of self-intersections<sup>44</sup>. Again, this energy barrier can be overcome more readily by mixed systems than pure ones. These inhomogeneities are smallest in the case of the gyroid and D surfaces. Clearly, in mixed systems, other surfaces can result. These theoretical expectations are spectacularly borne out by the experimental observations reported in this paper. *The range of bicontinuous microdomain patterns is much larger in mixed systems than in pure systems.*

The experimental data suggest that the formation of bicontinuous structures can also be promoted by using copolymers of more complex molecular architecture than the linear diblock molecules, such as tapered-block, graft-block and star-block copolymers. The tapered-block molecules suggest that the presence of hyperbolic interfaces is not confined to strongly-segregated molecules. The presence of bicontinuous phases in the graft-block case is being investigated theoretically. We believe that in this case, the unusual molecular geometry promotes the formation of bilayer-type laminated aggregates as schematically illustrated

in Figure 10. The large asymmetry in block volumes then forces the system to adopt a hyperbolic geometry. This proposal requires further analysis, but preliminary calculations are promising.

## CONCLUSIONS

We propose a new classification for the structures formed by the microphase separation of block or graft copolymers. According to the sign of Gaussian curvature ( $K$ ) of the interfaces, the structures can be classified into elliptic ( $K > 0$ ), parabolic ( $K = 0$ ) and hyperbolic ( $K < 0$ ) geometries. Bicontinuous and mesh morphologies belong to the hyperbolic realm: the continuity of domains is governed by the nature of the hyperbolic interface, containing both positive and negative sectional curvatures. Embedded triply periodic minimal surfaces, which are hyperbolic surfaces, offer useful geometric models for ordered bicontinuous microdomain structures with high symmetry. For example, the OBDD morphology is topologically identical to the D-surface. The existence of over 30 periodic minimal surfaces suggests the possibility of the existence of many different ordered bicontinuous microdomain morphologies, some examples of which are presented in this paper.

Two distinctive features are found in polymeric systems which exhibit bicontinuous microdomain structures. One is that they are polymer mixtures containing at least one block copolymer. Either a distribution in the block chain lengths, or the presence of additional homopolymers (of appropriate molecular weight), allows the adoption of variable interfacial curvatures—essential to hyperbolic forms in our space—whilst maintaining uniform segment density of the chains. Therefore, mixing two block copolymers and mixing homopolymers into block copolymers are simple ways to obtain bicontinuous nanodomain structures. The other feature of systems exhibiting the bicontinuous microdomain structures is that they are neat block copolymers with relatively complex molecular architectures. The resulting copolymer aggregate geometry is strongly constrained by the complex molecular architecture, effecting the formation of bicontinuous microdomain structures. However, sophisticated techniques are required to produce those polymers.

## ACKNOWLEDGEMENT

We are grateful to the late Professor Teruo Fujimoto, Nagaoka University of Technology, for providing TUN-1003 and YSF-12 samples. This work is supported in part by a Grant-in-Aid for Scientific Research on Priority Areas, 'Cooperative Phenomena in Complex Liquids', Ministry of Education, Science, Sports and Culture, Japan.

## REFERENCES

- 1 Hasegawa, H., Tanaka, H., Yamasaki, K. and Hashimoto, T. *Macromolecules* 1987, **20**, 1651
- 2 Thomas, E. L., Alward, D. B., Kinning, D. J., Martin, D. C., Handlin Jr., D. L. and Fetters, L. J. *Macromolecules* 1986, **19**, 2197
- 3 Hajduk, D. A., Harper, P. E., Gruner, S. M., Honeker, C. C.,



- Kim, G., Thomas, E. L. and Fetters, L. J. *Macromolecules* 1994, **27**, 4063
- 4 Hashimoto, T., Koizumi, S., Hasegawa, H., Izumitani, T. and Hyde, S. T. *Macromolecules* 1992, **25**, 1433
- 5 Skoulios, A. and Finaz, G. *J. Chim. Phys.* 1962, **59**, 473
- 6 Douy, A., Mayer, R., Rossi, J. and Gallot, B. *Mol. Cryst. Liq. Cryst.* 1969, **7**, 103
- 7 Hendus, H., Illers, K. and Ropte, E. *Kolloid-Z.* 1967, **216**, 110
- 8 Inoue, T., Soen, T., Kawai, H., Fukatsu, M. and Kurata, M. *Polym. Lett.* 1976, **14**, 847
- 9 Molau, G. E. in 'Block Polymers' (Ed. S. L. Aggarwal), Plenum, New York, 1970, p. 79
- 10 Folkes, M. J., Keller, A. and Odell, J. A. *J. Polym. Sci., Polym. Phys. Ed.* 1976, **14**, 847
- 11 Thomas, E. L., Alward, D. B., Henkee, C. S. and Hoffman, D. *Nature* 1988, **334**, 598
- 12 Nishikawa, Y., Hasegawa, H., Hashimoto, T. and Hyde, S. T. (in preparation)
- 13 Fogden, A. and Hyde, S. T. *Acta Crystallogr.* 1992, **A48**, 357
- 14 Koch, E. and Fischer, W. *Acta Crystallogr.* 1990, **A46**, 33
- 15 Schnering, H. G. and Nesper, R. *Angew. Chem.* 1987, **26**, 1059
- 16 Hasegawa, H., Nishikawa, Y., Koizumi, S., Hashimoto, T. and Hyde, S. T. 'Advanced Materials '93, II/A: Biomaterials, Organic and Intelligent Materials' (Eds H. Aoki, K. Segawa, T. Nishi, M. Hasegawa, I. Karube, T. Kajiyama and K. Takahashi), Elsevier, Amsterdam, 1994, pp. 225
- 17 Hasegawa, H., Nishikawa, Y., Hashimoto, T. and Hyde, S. T. (in preparation)
- 18 Winey, K. I., Thomas, E. L. and Fetters, L. J. *Macromolecules* 1992, **25**, 422
- 19 Spontak, R. J., Smith, S. D. and Ashraf, A. *Macromolecules* 1993, **26**, 956
- 20 Hashimoto, T., Kimishima, K. and Hasegawa, H. *Macromolecules* 1991, **24**, 5704
- 21 Hashimoto, T., Izumitani, T. and Ono, K. *Macromol. Symp.* 1995, **98**, 925
- 22 Iizuka, N., Hasegawa, H. and Hashimoto, T. (in preparation)
- 23 Xie, R., Yang, B. and Jiang, B. *Macromolecules* 1993, **26**, 7097
- 24 Wood, L. A. 'Polymer Handbook', 3rd Edn (Eds J. Brandrup and E. H. Immergut), Wiley, New York, 1989, p. V/7
- 25 Shibayama, M., Yang, H., Stein, R. S. and Han, C. C. *Macromolecules* 1985, **18**, 2179
- 26 Hashimoto, T., Tanaka, H. and Hasegawa, H. *Macromolecules* 1990, **23**, 4378
- 27 Koizumi, S., Hasegawa, H. and Hashimoto, T. *Makromol. Chem., Macromol. Symp.* 1992, **62**, 75
- 28 Schwier, C. E., Argon, A. S. and Cohen, R. E. *Polymer* 1985, **26**, 1985
- 29 Hadziioannou, G. and Skoulios, A. *Macromolecules* 1982, **15**, 267
- 30 Hashimoto, T., Yamasaki, K., Koizumi, S. and Hasegawa, H. *Macromolecules* 1993, **26**, 2895; 1994, **27**, 1562; Koizumi, S., Hasegawa, H. and Hashimoto, T. *Macromolecules* 1994, **27**, 4371
- 31 Riess, G., Schlienger, M. and Marti, S. *J. Macromol. Sci. Phys.* 1980, **B17**, 355
- 32 Shibayama, M., Hasegawa, H., Hashimoto, T. and Kawai, H. *Macromolecules* 1982, **15**, 274
- 33 Matsushita, Y., Yamada, K., Hattori, T., Fujimoto, T., Sawada, Y., Nagasawa, M. and Matsui, C. *Macromolecules* 1983, **16**, 10
- 34 Kudose, I. and Kotaka, T. *Macromolecules* 1984, **17**, 2325
- 35 Isono, Y., Tanisugi, H., Endo, K., Fujimoto, T., Hasegawa, H., Hashimoto, T. and Kawai, H. *Macromolecules* 1983, **16**, 5
- 36 Mogi, Y., Mori, K., Matsushita, Y. and Noda, I. *Macromolecules* 1992, **25**, 5408; 5412
- 37 Hasegawa, H., Sumitomo, T., Hashimoto, T. and Kawai, H. *Polym. Prepr., Jap. Soc. Polym. Sci.* 1983, **32**, 1695; Hasegawa, H., Sumitomo, T. and Hashimoto, T. (in preparation)
- 38 Stadler, R., Auschra, C., Beckmann, J., Krappe, U., Voigt-Martin, I. and Leiber, L. *Macromolecules* 1995, **28**, 3080
- 39 Aggarwal, S. L. *Polymer* 1976, **17**, 938
- 40 Herman, D. S., Kinning, D. J., Fetters, L. J. and Thomas, E. L. *Macromolecules* 1987, **20**, 2940
- 41 Se, K., Watanabe, O., Shibamoto, T. and Fujimoto, T. *Polym. Prepr., Div. Polym. Chem., Am. Chem. Soc.* 1988, **29**, 110
- 42 Tsukahara, Y., Nakamura, N., Hashimoto, T., Kawai, H., Nagaya, T., Sugiura, Y. and Tsuge, S. *Polymer J.* 1980, **12**, 455
- 43 Hyde, S. T., Fogden, A. and Ninham, B. W. *Macromolecules* 1993, **26**, 6782
- 44 Hyde, S. T., *J. Phys. (Coll.)* 1990, **C7**, 209